Development of 3D skin model and 3D skin infection model, as advanced testing tools for the bio-evaluation of antimicrobial biomaterials for wound healing

Development of 3D skin model and 3D skin infection model, as advanced testing tools for the bio-evaluation of antimicrobial biomaterials for wound healing

Scope of work

The aims & objectives of the current work and the tasks performed to accomplish these goals are presented schematically as following:

1. Aim: *In vitro* bio-evaluation (antibacterial activity and cytotoxicity) of novel antimicrobial polymeric biomaterials prepared under the project (https://hymedpoly.eu/) for wound healing applications (Chapter 07, 08, 09)
    A. Chitosan/Ag-doped mesoporous bioactive glass composite films (CS/ Ag-MBG)
    B. H_2O_2 being an active agent used in below mentioned H_2O_2 releasing hydrogel systems
    C. H_2O_2 releasing G/GO (glucose/glucose oxidase) containing PLGA (poly L-lactide-co-glycolide)-PEG (poly ethylene glycol)-PLGA copolymer hydrogels
    D. H_2O_2 releasing G/GO (glucose/glucose oxidase) containing HB-PEGDA (hyperbranched polyethylene glycol with numerous acrylate groups)/HA-SH (thiolated hyaluronic acid) hydrogels

2. Aim: Development of preliminary skin model (dermal-based) and *in vitro* assays in this 3D cell culture system (Chapter 02)
    A. Development of preliminary murine *in vitro* dermal construct (MDC)
    B. Development of human *in vitro* dermal construct (HDC)
        - Uniform distribution of cells inside a collagen type I-based extracellular matrix (ECM)
        - Viability of cells inside ECM over time
        - Effect of collagen type I concentration and cell seeding density on the development of dermal constructs
    C. Selection of the best suited assay to the respective cell type and 3D system
        - Evaluation of different cell viability assays (CellTiter-Blue®, RealTime-Glo™ MT, and CellTiter-Glo® from Promega)
        - Optimization of CellTiter-Glo® to adapt it to 3D systems

3. Aim: Development of epidermal skin model (Chapter 03)
    A. Development of reconstructed murine epidermis (RME)
    B. Development of reconstructed human epidermis (RHE)

C. Characterization (Histological staining for morphological analysis, immunohistochemistry (IHC) for proteins' tissue distribution analysis)
D. Future outlook: RHE and RME as key tools to understand the relevance of outcomes obtained from human- and animal-based systems reducing animal trials

4. Aim: Development of advanced tools for *in vitro* bio-evaluation of antimicrobial biomaterials for wound healing (Chapter 04 and Chapter 05)
    A. Development of three-dimensional dermal-epidermal based full-thickness human skin equivalent (HSE)
        - Optimization of 3D cell culture conditions
        - Characterization (Histological staining for morphological analysis, immunohistochemistry (IHC) for proteins' tissue distribution analysis, transmission electron microscopy (TEM) for ultrastructure analysis, scanning electron microscopy (SEM) for tissue architecture analysis, and wettability measurement for barrier function analysis)
    B. Development of *S. aureus* colonized human skin equivalent (c-HSE)
        - Development of a preliminary dermal infection system (c-HDC) using *S. aureus* and *P. aeruginosa*
        - Development of wounded HSEs by creating full-thickness incision
        - Development of c-HSE by inoculating *S. aureus* at wound site
        - Characterization of c-HSE applying light and electron microscopy to visualize bacterial interactions with HSE
        - Control experiments to examine bacterial interactions with intact HSE (without any incisional wounds)
            - Effect of low and high bacterial inoculum
            - Effect of time

5. Aim: Comparative 2D vs. 3D bio-evaluation of HSE and c-HSE as advanced tools for *in vitro* risk and antibacterial properties' assessment (Chapter 06)
    A. Selection of model materials: Ag containing antimicrobial wound dressings (Ag-dressings): namely PolyMem® Ag (Ferris), Biatain® Alginate Ag (Coloplast), Biatain® Ag (Coloplast), Atrauman® Ag (Hartmann) along with their controls without silver
    B. Bio-evaluation of aqueous solutions containing Ag^+ ions
        - Cytocompatibility evaluation of Ag^+ using 2D monolayer cell culture system (murine fibroblast & epidermal cell lines, and human primary fibroblasts and keratinocytes)
        - Cytocompatibility evaluation of Ag^+ using 3D cell culture system (HSE)

- MIC and MBC determination against wide range of bacterial strains
- Bacterial reduction (%) in tryptic soy broth (TSB) and simulated wound fluid (SWF) over time
- Antibacterial activity against colonized bacteria using infected skin model (c-HSE)

C. Bio-evaluation of Ag-dressings
- Cytocompatibility evaluation of Ag-dressings using 2D cell culture system (murine fibroblast & epidermal cell lines, and human primary fibroblasts and keratinocytes)
- Cytocompatibility evaluation of Ag-dressings using 3D cell culture system (HSE)
- Bacterial reduction (%) in tryptic soy broth (TSB) and simulated wound fluid (SWF) over time
- Antibacterial activity against colonized bacteria using infected skin model (c-HSE)

6. Aim: A general introduction and detailed literature review about 3D skin models – *In vitro* and *in vivo* applications and concepts (Chapter 01)

Abstract

Infected wounds still represent a great challenge in public health. With an increasing need for novel strategies to combat wounds colonized with resistant microbes, more reliable preclinical data are needed to bioanalyze antimicrobial polymeric biomaterials (AMPBs). A 3D human skin equivalent (HSE) and wound infection model (c-HSE) are highly demanded to serve as biomimetic system for the testing of AMPBs.

Initially "murine *in vitro* dermal construct" based on L929 cells was generated, leading to the development of "human *in vitro* dermal construct" (HDC) consisting of normal human dermal fibroblasts (NHDF) in rat tail tendon collagen type I. The models were characterised for cell viability and morphology as a function of time. Different viability assays (such as CellTiter-Blue®, RealTime-Glo™ MT, and CellTiter-Glo® from Promega) were evaluated to optimize the best suited assay to the respective cell type and 3D system (Chapter 02).

Then, in-house reconstructed human epidermis (RHE) based on normal human epidermal keratinocytes (NHEK) and reconstructed murine epidermis (RME) [1] based on COCA cells were developed with the aim to use them as test systems for biological evaluation and as basis to develop more complex 3D skin models. Developed RHE and RME would serve as key tools to understand the relevance of outcomes obtained from human- and animal-based systems reducing the animal trials (Chapter 03).

The human skin equivalent (HSE) was obtained having both a dermal and an epidermal compartment, by embedding NHDF in rat tail tendon collagen type I hydrogel (mimicking dermal extracellular matrix) and then seeding NHEK on it to generate the epidermis. Three-dimensional cell culture conditions (3D-CCs) based on commercially available serum/animal component-free and/or fully-defined media were applied to optimize the epidermal differentiation mimicking as closely as possible native human skin (NHS). The HSE was fully characterised for morphology analysis, immunohistochemistry (IHC) for proteins' tissue distribution analysis, transmission electron microscopy (TEM) for ultrastructure analysis, scanning electron microscopy (SEM) for tissue architecture analysis, and wettability measurement for barrier function analysis (Chapter 04).

Skin infection model was created by full-thickness incision and colonization with *S. aureus*. The *in vitro S. aureus* colonized HSE model was coded as c-HSE. The model was characterized for histology, immunohistochemistry, TEM, and SEM analysis. A preliminary dermal infection model (c-HDC) was also created by inoculating *S. aureus*, *P. aeruginosa, or S. aureus* + *P. aeruginosa* onto HDC (Chapter 05).

To validate the 3D systems, Ag^+ as an antibacterial agent and commercially available Ag containing antimicrobial wound dressings (Ag-dressings) [namely PolyMem Ag

(Ferris), Biatain® Alginate Ag (Coloplast), Biatain® Ag (Coloplast), Atrauman® Ag (Hartmann)] along with their controls without silver, were tested for cytocompatibility and antimicrobial properties using HSE and c-HSE. On the other hand, L929 cells, COCA cells, NHDF, and NHEK monolayer cell cultures were used as 2D cytocompatibility evaluation systems. Ag^{+} and Ag-dressings were evaluated for their antibacterial activities (e.g. MIC, MBC, CFU percentage reduction) against clinically relevant pathogens (*Staphylococcus aureus, Pseudomonas aeruginosa* etc.) under different growth media [tryptic soy broth (TSB) and simulated wound fluid (SWF)] over time to assess the effects of culture 'environment' on bacterial susceptibility to the toxic action of silver (Chapter 06).

The viability results of HDC showed that cells were viable inside the matrix. CellTiter-Glo® was found to be the optimal cell viability assay among the analysed ones. There is a need for more than one type of test methods to be applied in the 3D cell culture system based on different parameters, for example, NADPH enzyme activity, ATP content of cells, and /or DNA content to reveal all the different aspects of pathophysiologic reactions occurring in this system. This model was further advanced with more layers of skin to make a full thickness model (Chapter 02).

About RHE and RME, histological results showed the formation of fully organized and well-differentiated epidermal layers of stratum basale, spinosum, granulosum, and corneum. IHC analysis of RHE showed Keratin-14 (K14), a marker of early differentiation, as expressed by keratinocytes in stratum basale. Involucrin, a marker of terminal differentiation, was displayed by stratum corneum. (Chapter 03)

Histological results of HSE showed the formation of a dermal layer demonstrating NHDF with typical elongated filopodia-like morphology, that were uniformly distributed all along the dermal length. Histological results for epidermis showed characteristic multi-layered epidermis with well-differentiated layers of stratum basale, spinosum, granulosum, and corneum. IHC results showed that keratinocytes in basal layer were positive for Ki-67, demonstrating their active state of proliferation. Immunoreactivity for Keratins (K) indicated that K14 expression was displayed by keratinocytes in the basal layer while K10 (marker of early differentiation) was restricted to the supra-basal layers. Terminal differentiation was demonstrated as spotted expression of Filaggrin (Flg) and Loricin (Lor) in the sub-corneal and corneal layers of the epidermis. The basement membrane protein Laminin 5 (Lam 5) was displayed as a continuous line at Dermal-Epidermal Junction (DEJ). TEM revealed basement membrane with lamina lucida (LL), lamina densa (LD), regular hemidesmosomes and anchoring fibres. The epidermal layers showed abundant intracellular keratin filaments, desmosomes, and tight junction (TJ) between keratinocytes. SEM revealed the interwoven network and architecture of ECM with embedded dermal fibroblasts lying along collagen fibres; while epidermal layers appeared becoming increasingly flattened

as they moved to the surface. The contact angle of 82.5° ± 8.9° demonstrated the barrier function of HSE, which was highly comparable to the measurements of 90.0° ± 5.1° for NHS [2]. In this study, we successfully created an *in vitro* three-dimensional dermal-epidermal based interfollicular full-thickness human skin construct recapitulating the skin morphogenesis, epidermal differentiation, ultra-structure features, tissue architecture, and barrier function properties, closely imitating the properties of NHS and thus named as HSE (Chapter 04).

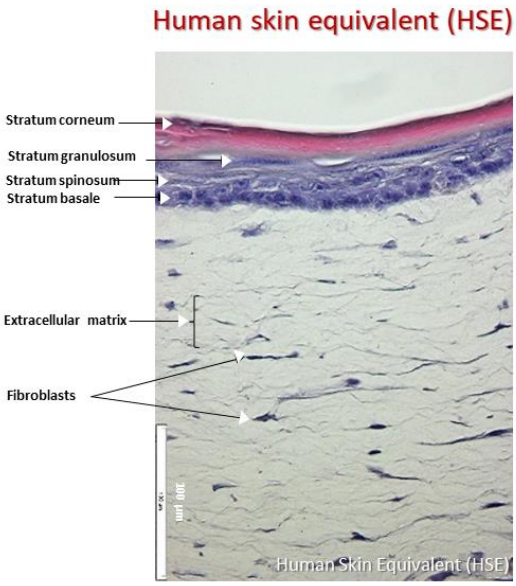

Figure 1 H & E stained histological image of HSE obtained from optimized 3D-CC-III was able to best recapitulate epidermal differentiation, morphogenesis and organization as found in NHS. HSE showed two structurally distinct layers of skin the outer epidermal layer, and the underlying thicker dermal layer. The epidermal part showed well differentiated layers of keratinocytes namely stratum basale, spinosum, granulosum, and corneum.

Bacterial aggregations and early biofilm formation were observed at wound site on c-HSE. Histological results demonstrated that bacterial colonization hindered the re-epithelialization process, when c-HSE was compared with uninfected wound control. TEM results revealed fibroblasts/keratinocytes cell lysis, *S. aureus* induced ECM degradation, and bacterial internalization by keratinocytes. SEM revealed grape-like bacterial clusters covered within extracellular polymeric substance at wound site in dermis and epidermis. The c-HDC results suggested that co-existence of *S. aureus* and *P. aeruginosa* may be significant for both bacterial colonization and pathogenicity in wounds. Histology revealed biofilm formation in all c-HDC groups, although it demonstrated denser colonized biofilm regions in c-HDC inoculated with *S. aureus* as compared to the c-HDC inoculated with *P. aeruginosa* (Chapter 05).

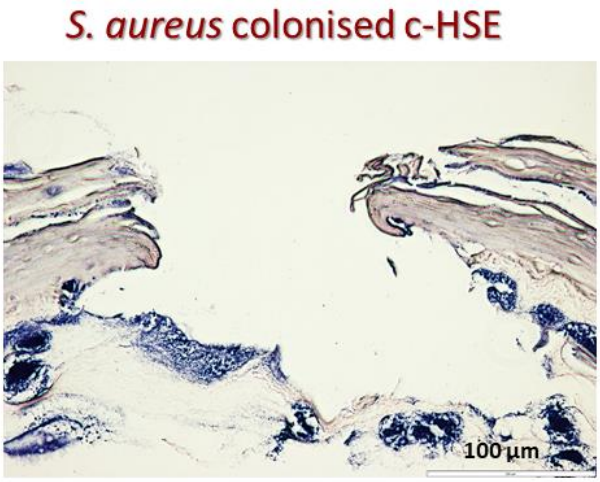

Figure 2 Histological cross-section of S. aureus colonized c-HSE.

Ag^+ showed IC50 of 2.3µg/mL, 10.8µg/mL, 10.3µg/mL and 11.8µg/mL in 2D monolayer cultures of L929, COCA, NHDF and NHEK, respectively, while IC50 was three times higher (34.2µg/mL) when using HSE. Tissue culture models indicated an 'environmental effect' on cytotoxicity, with decreased sensitivity to Ag^+ cytotoxicity for cells in 3D with respect to cells in 2D cultures. Ag^+ showed MIC in a range of 4.2-8.4µg/mL and MBC in a range of 4.2-33µg/mL against the tested Gram +ve and Gram -ve bacteria. The antibacterial activity of Ag^+ against *S. aureus* in TSB showed 99.99% reduction at T_{24h}, while it was not efficient when tested in SWF. This considerable variation indicated that antibacterial ability of Ag^+ was highly dependent on wound extracellular micro-environment, that could affect Ag^+ availability. Among tested Ag-dressings, the cytotoxicity tests using NHDF and NHEK indicated that silver released from Biatain® Ag (1% cell viability) and Biatain® Alginate Ag (53% cell viability) was lethal for both fibroblasts and keratinocytes. On the other hand, Biatain® Ag and Biatain® Alginate Ag demonstrated 77±21.8% and 92.5±10.6% cell viability with HSE, that was not significantly different than negative control. Biatain® Ag demonstrated 99.99% bacterial reduction against *S. aureus*, and Gram-ve (e.g. *P. aeruginosa*, and/or *E. coli*) in both TSB and SWF testing environments at all time points. On the contrary, Biatain® Alginate Ag showed 99% bacterial reduction against *S. aureus* and Gram-ve (e.g. *P. aeruginosa*) only in TSB but not in SWF environment at T_{24h}. When tested in a more complex *S. aureus* colonized HSE model (c-HSE), Biatain® Ag was still able to reduce bacterial burden and demonstrated significantly less (P=0.0085, **) Log CFU in Biatain® Ag treated c-HSE, while Biatain® Alginate Ag showed no significant reduction. These results demonstrated that as the cell viability decreased, the antibacterial effect increased. Among the tested Ag-dressings, Biatain® Ag was able to significantly reduce bacteria in c-HSE without significantly compromising cell viability of HSE in our advanced experimental set-ups. Other Ag-products were highly

compatible with cells but were not significantly lethal to bacteria. Also, it is worth noticing that the bio-evaluation outcomes were different in 2D monolayer vs. 3D cell culture systems. Additionally, results obtained from conventionally used microbial methods were different compared to those deriving from advanced c-HSE system. With an increasing need for reliable *in vitro* testing systems, we were successfully able to verify our advanced 3D models, to serve as a risk assessment platform for cytocompatibility and antibacterial properties. Moreover, results evidenced that a critical approach is required when using specific Ag-containing compounds/materials and Ag-dressings for wound care needs (Chapter 06).

HSE and c-HSE have great potential to develop even more complex skin models for testing skin treatment strategies, as these models allow the study of skin-pathogen interactions, and of novel targets for designing new antibacterial agents.

Additional efforts were addressed to the evaluation of the antibacterial properties and cytotoxicity of novel biomaterials:

(1) Chitosan/Ag-doped mesoporous bioactive glass composite films (CS/ Ag-MBG) (either using ordered or non-ordered MBGs) developed by ESR07-HyMedPoly (https://hymedpoly.eu/esr-7-bioactive-silica-glass/) intended for infected wound healing application (Chapter 7): namely "*CS/ non-ord. und. MBG", "CS/ non-ord. Ag-MBG", "CS/ ord. und. MBG",* and *"CS/ ord. Ag-MBG composites.*

(2) H_2O_2 releasing hydrogels developed by ESR01-HyMedPoly (https://hymedpoly.eu/esr-1-degradable-antibacterial-polyesters-and-composites/) as drug-free antibacterial systems for healing infected wounds (Chapter 8 and Chapter 9): HB-PEGDA (hyperbranched polyethylene glycol with numerous acrylate groups)/HA-SH (thiolated hyaluronic acid) hydrogels (namely 25U/L, 50U/L, 125U/L, 250U/L, 500U/L); and PLGA (poly L-lactide-co-glycolide)-PEG (poly ethylene glycol)-PLGA copolymer hydrogels (namely G10/E1000, G10/E2000, G20/E1000, G20/E2000), both containing glucose and glucose oxidase (G/GO).

Ag-doped composites (CS/ Ag-MBG) showed a decrease in CTB-derived L929 viability with respect to untreated control (as indicated by direct contact test) of approx. 60% for the *CS/ non-ord. Ag-MBG* and approx. 23% for the *CS/ ord. Ag-MBG composites*. However, in case of NHEK, the cytotoxic effects were reduced to approx. <20% for both Ag-doped composites as compared to their undoped composite counterparts. In the case of *CS/ ord. Ag-.MBG composite*, Ag release (0.9ppm for 03 days) could explain the cytotoxicity towards L929 cells, which were indeed more sensitive to silver than were NHEK. However, the low L929 cell viability in contact with *CS/ non-ord. Ag-MBG composite* could not be correlated to Ag release (0.0ppm for 03 days), but rather to other factors, such as surface topography, porosity, particle size distribution, wettability, chemical, and mechanical properties. Additionally, Ag release was evaluated in SBF,

while cell tests were performed in culture medium: probably the interaction of the substrate with SBF during Ag release tests affected the kinetics of Ag release. This means that the measured release data did not reproduce Ag release in culture medium during cell tests. In support to this hypothesis, both Ag-doped composites demonstrated antibacterial activity against tested bacteria, and zone of inhibition (ZOI) values were found similar between *CS/ non-ord. Ag-MBG* and *CS/ ord. Ag-MBG composites.* Thus, due to antibacterial, cytocompatibility, and water retaining properties, in general, Ag-doped composites especially *CS/ ord. Ag-MBG composite* might have a potential for wound application (Chapter 07).

The cytotoxic effects of 10% (w/w) HB-PEGDA/1% (w/w) HA-SH hydrogel samples encapsulated with glucose (2.5%, w/w) and GO at various concentrations (25U/L, 50U/L, 125U/L, 250U/L, 500U/L), demonstrated that the effect was highly dependent on the type of test procedure [direct contact, indirect contact, and adapted direct contact methods (where samples were pre-treated in cell culture medium)] as well as concentration of encapsulated GO. For example, under direct contact test, hydrogels with GO ≤50U/L demonstrated the minimum cytotoxic effect of ~25% with NHDF. On the other hand, under indirect contact test, 250U/L GO hydrogels demonstrated approx.~≤32% cytotoxicity with both NHDF and NHEK. However, under adapted direct contact test, 250U/L GO hydrogels demonstrated approx. ≤13% cytotoxicity with both NHDF and NHEK. H_2O_2 releasing hydrogels, in general, performed better against Gram +ve than against Gram -ve bacteria where hydrogels demonstrated antibacterial activity at comparatively higher GO concentrations. H_2O_2 releasing hydrogels prepared using 250 U/L GO demonstrated a strong antibacterial effect against a wide range of wound associated pathogens. H_2O_2 released from hydrogels at high GO concentrations could be reduced by bacterial burden and wound exudate, decreasing the possible direct cytotoxic effects towards cells. Ideally, burst H_2O_2 release could reduce bacterial burden at initial stages, followed by a sustained lower H_2O_2 release to prevent bacterial re-colonization (Chapter 09).

As a preliminary H_2O_2 releasing hydrogel system, PLGA (poly L-lactide-co-glycolide)-PEG (poly ethylene glycol)-PLGA copolymer was encapsulated with G/GO [G10(w/w) / E1000(U/L), G10/E2000, G20/E1000, and G20/E2000]. H_2O_2 releasing hydrogels severely affected cell metabolic activity, cell membrane integrity, and cell morphology at all tested G/GO concentrations. Based on that, an optimization of the G/GO relative amount would be needed as to optimize H_2O_2 release (Chapter 09-Appendix D).

H_2O_2 alone as an active agent without released from hydrogels was also investigated at range of 20mM-0.1µM and the cell viability results showed an IC50 of 75.6µM with L929 cells in our experimental set-up, while the MIC and MBC (99.9% bacterial reduction) against *S. aureus* was measured as 500µM. The redox environment at wound site might induce wound healing by promoting cells (Chapter 08).

As a conclusion, H_2O_2 as an antibacterial agent should be used carefully for wound cleaning to kill pathogens, as at high concentrations it might damage newly proliferating cells surrounding the wound area. This should be taken into consideration while choosing H_2O_2 based antibacterial wound dressings. Moreover, the suitability of a certain hydrogel matrix system for G/GO encapsulation, the uniform distribution of GO & its activity inside this polymer matrix, and the susceptibility of covalent linkages of polymers towards peroxidation damage are important to be considered and investigated rationally.

References

1. Segrelles, C., et al., *Establishment of a murine epidermal cell line suitable for in vitro and in vivo skin modelling.* BMC dermatology, 2011. 11(1): p. 9.
2. Casale, C., et al., *Endogenous human skin equivalent promotes in vitro morphogenesis of follicle-like structures.* Biomaterials, 2016. 101: p. 86-95.